

Persistent nonequilibrium effects in generalized Langevin dynamics of nonrelativistic and relativistic particles

Weiguo Chen,¹ Carsten Greiner,² and Zhe Xu ^{*1}

¹*Department of Physics, Tsinghua University and Collaborative Innovation Center of Quantum Matter, Beijing 100084, China*

²*Institut für Theoretische Physik, Johann Wolfgang Goethe-Universität Frankfurt, Max-von-Laue-Strasse 1, 60438 Frankfurt am Main, Germany*

Persistent nonequilibrium effects such as the memory of the initial state, the ballistic diffusion, and the break of the equipartition theorem and the ergodicity in Brownian motions are investigated by analytically solving the generalized Langevin equation of nonrelativistic Brownian particles with colored noise. These effects can also be observed in the Brownian motion of relativistic particles by numerically solving the generalized Langevin equation for specially chosen memory kernels. Our analyses give rise to think about the possible anomalous motion of heavy quarks in relativistic heavy-ion collisions.

I. INTRODUCTION

The Brownian motion is a famous stochastic process exhibiting the relationship between the fluctuation and the dissipation in statistical physics. Mathematically, it is described by the Langevin equation. The common knowledge from text books by solving the Langevin equation is that the Brownian motion is a random motion of the Brownian particle in a fluid or gas. In the long-time limit and with the ensemble average, the Brownian particle will reach the thermal equilibrium with the matter where it is suspended and diffuse linearly with time. On the other hand, for specific interactions between the Brownian particle and the particles which the matter is made of, the fluctuation as well as the dissipation correlate with their former values in the motion. The current motion is determined by the motion in the past by means of the memory kernel in the generalized Langevin equation. This memory property can give rise to a different diffusion from the linear one, called the anomalous diffusion [1–11], and break the equipartition theorem and the ergodicity [12, 13]. Previous research motivates us to make a systematical study of classifying memory kernels according to the resulting different behaviors in Brownian motions. In this way we try to find out the general behavior of the thermal equilibrium, diffusion, and ergodicity of the Brownian particle for any kind of memory kernel.

The motion of heavy quarks in the quark-gluon plasma produced in relativistic heavy-ion collisions has been considered a Brownian motion in the QCD matter and described by the relativistic form of the Langevin equation [14–16]. However, this treatment cannot simultaneously explain the experimental data of the energy loss and the collective flow of hadronic particles stemming from heavy quarks [14, 17–27]. Could an anomalous motion of heavy quarks explain the data? To answer this question, one has to first verify that the persistent nonequilibrium ef-

fects that can occur in the motion of nonrelativistic Brownian particles can also occur in the motion of relativistic Brownian particles. This is another goal of this paper. The verification is not trivial, since the relativistic Langevin equation is not a linear equation and cannot be solved analytically.

The paper is organized as follows. In Sec. II, we analytically solve the generalized Langevin equation of nonrelativistic Brownian particles by employing the Laplace technique. The memory kernels are classified into four categories. All the behaviors are normal in the first category. The diffusion is normal. The equipartition theorem and the ergodicity hold. In the second category, the memory effect occurs, the diffusion is ballistic, and the equipartition theorem and ergodicity are broken. In the third category, besides the memory effect and the break of the ergodicity, an oscillating behavior appears, which brings the Brownian particle out of and back to the equilibrium periodically. In the fourth category, subdiffusion and superdiffusion are discussed. We give examples of the memory kernels and present the analytical results of the averaged kinetic energy, displacement squared, and the velocity correlation function of the Brownian particle. In Sec. III, the Langevin equation of relativistic Brownian particles is solved numerically for the memory kernels given in the previous section. Except for the oscillation, other persistent nonequilibrium effects are also seen in relativistic Brownian motions. We give a summary in Sec. IV and show the details in Laplace transformations in the Appendix.

II. THE LANGEVIN EQUATION OF NONRELATIVISTIC BROWNIAN PARTICLES

A. Analytical solutions

The motion of nonrelativistic Brownian particles is described by the generalized Langevin equation

$$m\dot{\mathbf{v}}(t) = - \int_0^t dt' \Gamma(t-t') \mathbf{v}(t') + \boldsymbol{\xi}(t) \quad (1)$$

*xuzhe@mail.tsinghua.edu.cn

with

$$\langle \xi_i(t)\xi_j(t') \rangle = \delta_{ij}A(t-t'). \quad (2)$$

Here we set the initial time to be 0. The generalized Langevin equation describes a non-Markov process. The interactions of the Brownian particle with the molecules of the matter at earlier times also affect the current change of momentum. This is, on the one hand, revealed by the memory kernel $\Gamma(t-t')$. On the other hand, the noise ξ at the current time correlates with those at earlier times as $A(t-t')$. Since the Fourier transform of $A(t-t')$ to the frequency space has a structure other than a constant, such noise is denoted as colored noise. The fluctuation-dissipation theorem reads

$$A(t-t') = k_B T \Gamma(t-t'), \quad (3)$$

according to the second kind of Kubo's law [28]. We note that the correlation function $A(t-t')$ [also $\Gamma(t-t')$] is such kind of function, which Fourier transforms are non-negative [29, 30].

Particularly, for $A(t-t') = \alpha\delta(t-t')$ and $\Gamma(t-t') = 2\gamma\delta(t-t')$, the generalized Langevin equation, Eq. (1), reduces to

$$m\dot{\mathbf{v}} = -\gamma\mathbf{v} + \boldsymbol{\xi}, \quad (4)$$

with

$$\langle \xi_i(t)\xi_j(t') \rangle = \delta_{ij}\alpha\delta(t-t'). \quad (5)$$

This noise is called white noise. The fluctuation-dissipation theorem reduces to

$$\alpha = 2k_B T \gamma. \quad (6)$$

The question now is whether the Brownian particle under colored noise will relax to the thermal equilibrium state. In the following, we will show that the answer to this question depends on the actual functional form of the memory kernel $\Gamma(t-t')$. For some classes of $\Gamma(t-t')$, the Brownian particle will not relax to the thermal equilibrium with the surrounding matter. Moreover, even in the long-time limit the Brownian particle still keeps the memory on its initial state, its diffusion shows an anomalous behavior, and the ergodicity is broken.

Performing the Laplace transformation of Eq. (1), we obtain

$$ms\mathbf{v}(s) - m\mathbf{v}(0) = -\Gamma(s)\mathbf{v}(s) + \boldsymbol{\xi}(s), \quad (7)$$

where s is defined in the complex space. We then have

$$\mathbf{v}(s) = \frac{\mathbf{v}(0) + \frac{1}{m}\boldsymbol{\xi}(s)}{s + \frac{1}{m}\Gamma(s)}. \quad (8)$$

Defining the response function in the Laplace space as

$$G(s) = \frac{1}{s + \frac{1}{m}\Gamma(s)}, \quad (9)$$

Eq. (8) is rewritten to

$$\mathbf{v}(s) = \mathbf{v}(0)G(s) + \frac{1}{m}G(s)\boldsymbol{\xi}(s). \quad (10)$$

We then perform the inverse Laplace transformation of Eq. (10) and obtain

$$\mathbf{v}(t) = \mathbf{v}(0)G(t) + \frac{1}{m}\int_0^t dt' G(t-t')\boldsymbol{\xi}(t'). \quad (11)$$

At $t = 0$, we find $G(t=0) = 1$. With Eq. (11), we have

$$\begin{aligned} \langle v^2 \rangle(t) &= v^2(0)G^2(t) + \frac{1}{m^2}\int_0^t dt' G(t-t') \\ &\quad \times \int_0^t dt'' G(t-t'') \langle \boldsymbol{\xi}(t'') \cdot \boldsymbol{\xi}(t') \rangle \\ &= v^2(0)G^2(t) + \frac{3k_B T}{m^2}\int_0^t dt' G(t-t') \\ &\quad \times \int_0^t dt'' G(t-t'')\Gamma(t''-t'). \end{aligned} \quad (12)$$

After some steps, which can be found in the Appendix, we get the final result [11, 31, 32]:

$$\langle v^2 \rangle(t) = v^2(0)G^2(t) + \frac{3k_B T}{m} [1 - G^2(t)]. \quad (13)$$

Before we present the results of $\langle v^2 \rangle(t)$ for some chosen memory kernels, we now discuss generally the long-time behavior of $\langle v^2 \rangle$ and give the answer whether the Brownian particle will relax to the thermal state. From Eq. (13), it is obvious that if the Brownian particles are initially in the thermal state, i.e., $\langle v^2 \rangle(0) = 3k_B T/m$, they always stay in the thermal state, $\langle v^2 \rangle(t) = 3k_B T/m$, regardless of the actual form of the memory kernel. For the case that the Brownian particles are initially out of thermal equilibrium, they will approach the thermal state, only if $G(t \rightarrow \infty) = 0$. In the following, we examine $G(t \rightarrow \infty)$ for the nonthermal initial state of Brownian particles.

Performing the inverse Laplace transformation, we have

$$\begin{aligned} G(t) &= L^{-1}[G(s)] = \frac{1}{2\pi i} \int_{\beta-i\infty}^{\beta+i\infty} ds G(s)e^{st} \\ &= \frac{1}{2\pi i} \int_{\beta-i\infty}^{\beta+i\infty} ds \frac{1}{s + \frac{1}{m}\Gamma(s)} e^{st}. \end{aligned} \quad (14)$$

The integral area should be chosen to ensure that the integral is convergent. So, we choose the left half of the complex plane with respect to the imaginary axis (the real part is negative). Along the semicircle with the infinite radius the integral vanishes. Suppose $G(s)$ has n single poles $s_j = \sigma_j + i\omega_j$, $j = 1, 2, \dots, n$. $G(s)$ can be written to

$$G(s) = \sum_{j=1}^n \frac{a_j}{s - s_j}, \quad (15)$$

where

$$a_j = \lim_{s \rightarrow s_j} (s - s_j)G(s). \quad (16)$$

Thus, we obtain

$$G(t) = \sum_{j=1}^n a_j e^{s_j t} \quad (17)$$

according to the residue theorem. The case that $G(s)$ has branch points will be discussed later in this subsection.

To discuss the general behaviors of the Brownian particle for any kind of memory kernel, we classify memory kernels according to the position of poles and branch points of $G(s)$. First, we consider poles only. If the poles are located in the left half of the complex plane and not on the imaginary axis, the real part of $e^{s_j t}$ is $e^{\sigma_j t}$ with a negative σ_j . Therefore, we have $G(t \rightarrow \infty) = 0$. In this case, the Brownian particle will relax to the thermal equilibrium with the surrounding matter. For example, we choose [33, 34]

$$\Gamma_1(t - t') = \frac{\gamma}{2\tau} e^{-\frac{|t-t'|}{\tau}}. \quad (18)$$

Its Laplace transform is

$$\Gamma_1(s) = \frac{\gamma}{2(1 + s\tau)}. \quad (19)$$

$G_1(s)$ has two poles located in the left half of the complex plane and not on the imaginary axis. Therefore, $G_1(t \rightarrow \infty) = 0$.

Second, we consider the case that only one of the poles is located on the imaginary axis and specially at $s = 0$. In this case, it should be $\Gamma(s = 0) = 0$ [see Eq. (9)]. We have $G(t \rightarrow \infty) = a_1$, where

$$\begin{aligned} a_1 &= \lim_{s \rightarrow 0} sG(s) = \lim_{s \rightarrow 0} \frac{s}{s + \frac{1}{m}\Gamma(s)} \\ &= \frac{1}{1 + \frac{1}{m} \frac{d\Gamma(s)}{ds} \Big|_{s=0}} \equiv \frac{1}{1 + Q} \end{aligned} \quad (20)$$

with

$$\begin{aligned} Q &= \frac{1}{m} \frac{d}{ds} \int_0^\infty dt \Gamma(t) e^{-st} \Big|_{s=0} \\ &= -\frac{1}{m} \int_0^\infty dt \Gamma(t) t. \end{aligned} \quad (21)$$

We see that $G(t \rightarrow \infty)$ is nonzero. The equipartition theorem is broken and the Brownian particle will relax to a certain state, but not to the thermal equilibrium with the surrounding matter. In addition, from Eq. (13) we see that the term $v^2(0)G^2(t)$ contributes to $\langle v^2 \rangle(t)$, which indicates that in the long-time limit the Brownian particle still keeps the memory of its initial state. This is the memory effect.

From Eq. (13), we also see that $G(t)$ is smaller than 1, because $\langle v^2 \rangle$ is always positive, also for $v(0) = 0$. If $v(0) = 0$, the kinetic energy $m \langle v^2 \rangle / 2$ will reach a smaller value than that from the equipartition theorem. $G(t) < 1$ also leads to $a_1 < 1$ and thus $Q > 0$. We realize that in this case negative correlations, $\Gamma(t) < 0$ at some time interval, will occur. This indicates that the mean force does not always decelerate the Brownian particle. It will also accelerate the Brownian particle. This might be the physical reason, why the Brownian particle cannot approach the thermal equilibrium with the surrounding matter.

We choose, for example [33],

$$\Gamma_2(t - t') = \frac{\gamma}{4\tau} \left(1 - \frac{|t - t'|}{\tau} \right) e^{-\frac{|t-t'|}{\tau}}, \quad (22)$$

which falls to be negative at $t - t' = \tau$ and approaches 0 at large $t - t'$ from the negative side. This correlation resembles that for studying the non-Markov dissipative evolution of the chiral fields [30]. The Laplace transform is

$$\Gamma_2(s) = \frac{\gamma s \tau}{4(1 + s\tau)^2}. \quad (23)$$

$G_2(s)$ has one pole at $s = 0$ and the other two poles in the left half of the complex plane and not on the imaginary axis.

Third, some poles are located on the imaginary axis, but not at $s = 0$. These poles appear in pairs symmetric to $s = 0$, $s_{1,2} = \pm i\omega_1$, for instance. We can write $G(s)$ to the form

$$G(s) = \sum_{j=1}^k \left(\frac{a_j}{s - i\omega_j} + \frac{a_j^*}{s + i\omega_j} \right) + \sum_{j=2k+1}^n \frac{a_j}{s - s_j}. \quad (24)$$

We obtain $G(\infty) = \lim_{t \rightarrow \infty} \sum_{j=1}^k 2[Re(a_j) \cos(\omega_j t) - Im(a_j) \sin(\omega_j t)]$. The oscillations of $G(t)$ are not damped in the long-time limit due to the absence of the real part of the poles. In this case, the Brownian particle will not even approach a steady state. On the other hand, $G(t)$ oscillates across zero. When $G(t)$ is zero, the Brownian particle is at the thermal equilibrium. So, in the long-time limit, the Brownian particle goes out of and returns to the thermal equilibrium circularly. An example, Γ_3 , will be given later. We note that kernels of the second and third classes were not discussed in Ref. [35], where the Fourier transformation was used to solve the generalized Langevin equation.

Fourth, we consider the memory kernels having the following form at $s \rightarrow 0$ [11]:

$$\lim_{s \rightarrow 0} \Gamma_4(s) = \gamma(s\tau)^{\lambda-1}, \quad (25)$$

where λ is a fractional number. With this, $G_4(s)$ has the branch points at $s = 0$. For $G(s)$ having branch points, but other than Eq. (25), we postpone to further

investigations. Putting Eq. (25) into Eq. (14), we obtain

$$G_4(t) = \frac{1}{2\pi i} \int d(st) \frac{(st)^{1-\lambda}}{(st)^{2-\lambda} + \frac{\gamma\tau}{m} \left(\frac{t}{\tau}\right)^{2-\lambda}} e^{st}. \quad (26)$$

In the long-time limit and $\lambda < 2$, $G_4(t)$ can be solved by using asymptotic expansions [36]. For $0 < \lambda < 2$, it is

$$G_4(t) \sim \left(\frac{t}{\tau}\right)^{\lambda-2} \rightarrow 0. \quad (27)$$

The Brownian particle will relax to the thermal equilibrium with the surrounding matter and the equipartition theorem of energy holds. For $\lambda < 0$, we have

$$G_4(t) \sim \sum_n \left(\frac{t}{\tau}\right)^{\frac{2-\lambda}{n}} \exp \left[\exp \left(\frac{2n\pi i}{2-\lambda} \right) \frac{t}{\tau} \right], \quad (28)$$

which is complex and divergent for $t \rightarrow \infty$. Thus, this case is not physical. At last, for $\lambda > 2$, $(t/\tau)^{2-\lambda}$ goes to 0 in the long-time limit and thus, $s = 0$ becomes a pole position [see Eq. (26)]. The persistent nonequilibrium effects are the same as those discussed before for the class of memory kernels with a pole at $s = 0$.

We present now the analytical results of $G(t)$ for chosen memory kernels $\Gamma(t-t')$. For $\Gamma_1(t-t')$ [see Eq. (18)], we obtain results for two cases. If $B \equiv \sqrt{1-2\gamma\tau/m}$ is real, we have

$$G_{11}(t) = \left[\cosh \left(B \frac{t}{2\tau} \right) + \frac{1}{B} \sinh \left(B \frac{t}{2\tau} \right) \right] e^{-\frac{t}{2\tau}}. \quad (29)$$

If B is pure imaginary, we define $B' = -iB = \sqrt{2\gamma\tau/m-1}$ and have

$$G_{12}(t) = \left[\cos \left(B' \frac{t}{2\tau} \right) + \frac{1}{B'} \sin \left(B' \frac{t}{2\tau} \right) \right] e^{-\frac{t}{2\tau}}. \quad (30)$$

For $\Gamma_2(t-t')$ [see Eq. (22)], we obtain

$$G_2(t) = \frac{1}{1+C} + \left[\frac{C}{1+C} \cos \left(\sqrt{C} \frac{t}{\tau} \right) + \frac{\sqrt{C}}{1+C} \sin \left(\sqrt{C} \frac{t}{\tau} \right) \right] e^{-\frac{t}{\tau}}, \quad (31)$$

where $C = \gamma\tau/(4m)$.

For the third case, we choose

$$\Gamma_3(t-t') = \gamma \frac{1 + \omega^2 \tau^2}{2\tau(\omega^2 \tau^2 + 1 - \epsilon)} [1 - \epsilon \cos(\omega|t-t'|)] e^{-\frac{|t-t'|}{\tau}}, \quad (32)$$

which has a oscillating disturbance. The amplitude ϵ should be

$$\epsilon \leq \frac{4}{W} \left[\sqrt{(W+1)(W+4)} - W - 2 \right] \quad (33)$$

with $W = \omega^2 \tau^2$, so the Fourier transform of $\Gamma_3(t-t')$ is non-negative. The Laplace transform of $\Gamma_3(t-t')$ is

$$\Gamma_3(s) = \gamma' \left[\frac{1}{1+s\tau} - \epsilon \frac{1+s\tau}{W+(1+s\tau)^2} \right], \quad (34)$$

where

$$\gamma' = \gamma \frac{W+1}{2(W+1-\epsilon)}. \quad (35)$$

$G_3(s)$ has four poles. Two of them are located in the left half of the complex plane, while another two poles are on the imaginary axis, when γ' is the solution of the equation

$$2(1-\epsilon)^2 \tau^2 \gamma'^2 + m\tau[(1-\epsilon)(8+5W) - 9W]\gamma' + 2m^2(W+1)(W+4) = 0. \quad (36)$$

The condition that the above equation has a solution is

$$\epsilon \geq \frac{4}{W} \left[\sqrt{(W+1)(W+4)} - W - 2 \right]. \quad (37)$$

Together with condition (33), we have

$$\epsilon = \frac{4}{W} \left[\sqrt{(W+1)(W+4)} - W - 2 \right]. \quad (38)$$

We see that ϵ is fixed for given $\omega\tau$. With this, we obtain

$$\frac{\gamma\tau}{m} = \frac{2(W+1-\epsilon)}{W+1} \frac{\sqrt{(W+1)(W+4)}}{1-\epsilon}. \quad (39)$$

The strength of the memory kernel, γ , is not a free parameter. It relates to the frequency of the oscillation ω , the decay timescale τ , and the mass of the Brownian particle m . This indicates that the case that poles are located on the imaginary axis (not at the origin) hardly occurs. This is different from $\Gamma_1(t-t')$ and $\Gamma_2(t-t')$, in which γ and τ are free parameters. After a lengthy derivation, we obtain

$$G_3(t) = \frac{1}{1 + \frac{1}{2}\sqrt{\frac{W+1}{W+4}}} \cos \left(\sqrt{\frac{Z-6W-3}{6}} \frac{t}{\tau} \right) + \frac{1}{1 + 2\sqrt{\frac{W+4}{W+1}}} \left[\frac{3\sqrt{3}}{\sqrt{Z}} \sin \left(\frac{\sqrt{Z}}{2\sqrt{3}} \frac{t}{\tau} \right) + \cos \left(\frac{\sqrt{Z}}{2\sqrt{3}} \frac{t}{\tau} \right) \right] e^{-\frac{3t}{2\tau}}, \quad (40)$$

where $Z = 8W + 4\sqrt{(W+1)(W+4)} + 5$.

From the dependence of G_{11} on B , G_{12} on B' , G_2 on C , and G_3 on W , we realize that all G 's, as functions of t/τ , are fixed by the only parameter $\gamma\tau/m$. The same is also for the memory kernels Γ_1 , Γ_2 , and Γ_3 multiplied by τ^2/m . Figure 1 shows the chosen memory kernels (times τ^2/m) and the respective G 's as functions of t/τ . The curves of Γ_1 with $B' = 3$ and Γ_3 with $W = 2$ are divided by 10. We do not give examples of memory kernels in the last category because $G(t)$ cannot be solved analytically.

In Fig. 2, we show the time evolution of the average kinetic energy of the Brownian particle, $\langle E_k \rangle = m \langle v^2 \rangle / 2$, scaled by $k_B T$, according to Eq. (13). The

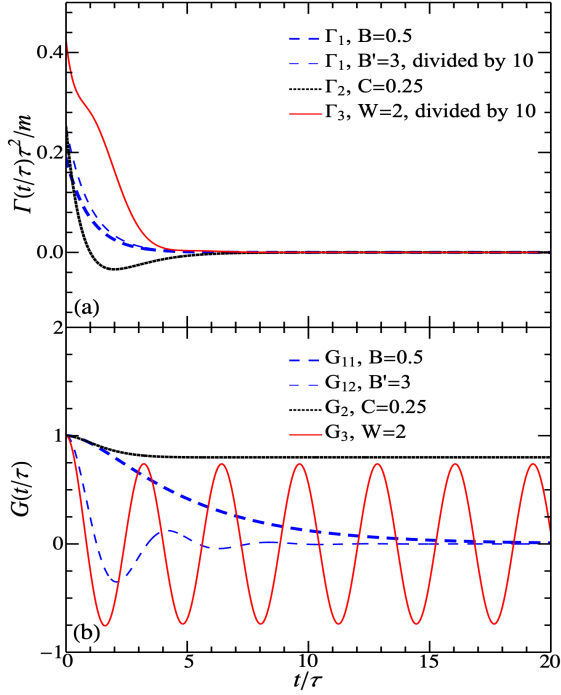


FIG. 1: Examples of the memory kernels (upper panel) and the response functions (lower panel) as functions of t/τ . The memory kernels are multiplied by τ^2/m .

initial momentum of the Brownian particle, $p_0 = mv(0)$, is set to be zero. The solid curve depicts the result under white noise, where $G(t) = e^{-t/\tau}$. Here τ denotes m/γ and thus $\gamma\tau/m = 1$. Other curves depict the results under colored noise with the memory kernels given before and shown in Fig. 1. We see that the averaged kinetic energy of the Brownian particle under white noise and colored noise with Γ_1 approaches the value according to the equipartition theorem. This corresponds to the case that the poles of the response function $G(s)$, the Laplace transform of $G(t)$, locate in the left half of the complex plane and not on the imaginary axis. For the case with Γ_2 , where one of the poles of $G(s)$ is at the origin, $s = 0$, the averaged kinetic energy is less than the value according to the equipartition theorem. Finally, for the case with Γ_3 , where two of the poles of $G(s)$ are on the imaginary axis, the averaged kinetic energy oscillates. At the peaks, it reaches the value according to the equipartition theorem. The difference between the peak and the trough equals to the square of the amplitude of the first term of $G_3(t)$ times $3/2$ [see Eqs. (40) and (13)] and varies between $24/25$ for $W \rightarrow 0$ and $2/3$ for $W \rightarrow \infty$.

By comparing with Fig. 2, the memory effect can be observed in Fig. 3, where the initial momentum is set to be $p_0 = \sqrt{mk_B T}$. Again, in the long-time limit, the averaged kinetic energy of the Brownian particle under white noise and colored noise with Γ_1 approaches the value according to the equipartition theorem. In these

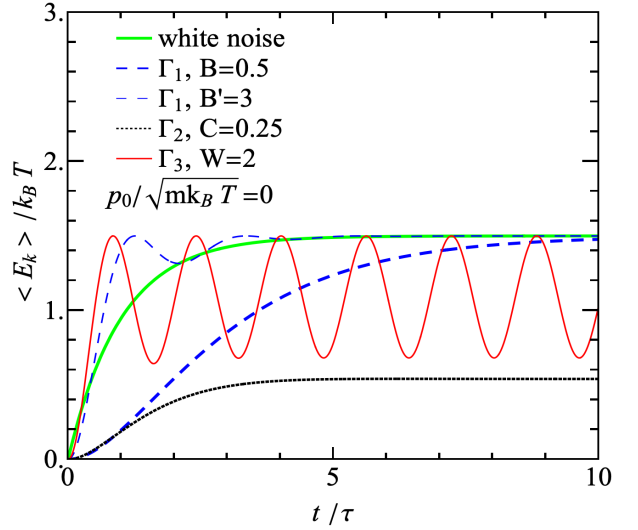


FIG. 2: The time evolution of the average kinetic energy of the Brownian particle under white noise and colored noise with the chosen memory kernels. The initial momentum of the Brownian particle is set to be zero.

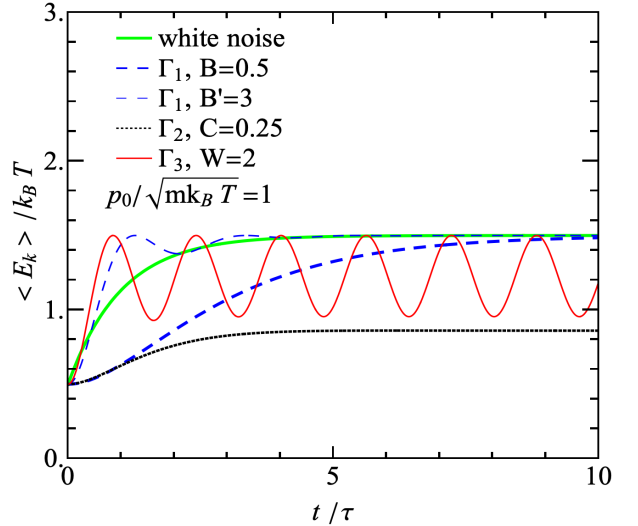


FIG. 3: Same as Fig. 2. The initial momentum is set to be $p_0 = \sqrt{mk_B T}$.

cases, no memory effect is expected. From the results with Γ_2 and Γ_3 , we do see the memory effect. The larger the initial momentum, the larger the averaged kinetic energy of the Brownian particle with Γ_2 in the long-time limit. In the case of Γ_3 , for $p_0 < \sqrt{3mk_B T}$, the averaged kinetic energy at long times reaches the value according to the equipartition at the peaks of the oscillation. The difference between the peak and the trough is decreasing to zero, when the initial momentum is increasing from zero to $\sqrt{3mk_B T}$. For $p_0 > \sqrt{3mk_B T}$, the averaged kinetic energy at long times reaches the value according to the equipartition at the troughs of the oscillation. The difference between the peak and the trough is increasing

for the increasing initial momentum.

We now study the diffusion behavior of the Brownian particle with colored noise. Since $\mathbf{v} = \dot{\mathbf{x}}$, the Langevin equation, Eq. (1), can be rewritten to

$$m\ddot{\mathbf{x}} = - \int_0^t dt' \Gamma(t-t') \dot{\mathbf{x}}(t') + \boldsymbol{\xi}(t). \quad (41)$$

Performing the Laplace transformation to Eq. (41) and proceeding the same steps such as solving Eq. (1), we obtain the analytical results of $\langle (\Delta \mathbf{x})^2 \rangle$,

$$\langle (\Delta \mathbf{x})^2 \rangle(t) = \mathbf{v}^2(0)H^2(t) + \frac{3k_B T}{m} \left[2 \int_0^t dt' H(t-t') - H^2(t) \right], \quad (42)$$

where

$$H(t) = L^{-1}[H(s)] \text{ and } H(s) = \frac{1}{s}G(s). \quad (43)$$

Since $H(t=0) = 0$, we have $\dot{H}(t) = G(t)$. For the known $G(t)$, the analytical results of $\langle (\Delta \mathbf{x})^2 \rangle(t)$ can be easily calculated. In the following, we discuss its long-time behavior.

- (i) For the case that the poles of $G(s)$ are located in the left half of the complex plane and not on the imaginary axis such as for white noise and colored noise with Γ_1 , $H(s)$ has an additional pole at $s=0$ due to Eq. (43). In the long-time limit, we have $H(t) \rightarrow G(s=0)$ and thus $\langle (\Delta \mathbf{x})^2 \rangle(t) \rightarrow 6k_B T G(s=0)t/m$, which is proportional to t . This is the normal diffusion. For white noise, $G(s=0) = m/\gamma$, we get $\langle (\Delta \mathbf{x})^2 \rangle(t) \rightarrow 6k_B T t/\gamma = 6Dt \sim t$, where D is the diffusion constant. For Γ_1 , $G_1(s=0) = 2m/\gamma$, we get $\langle (\Delta \mathbf{x})^2 \rangle(t) \rightarrow 12k_B T t/\gamma \sim t$. Therefore,

$$\frac{m \langle (\Delta \mathbf{x})^2 \rangle}{k_B T \tau^2} \Big|_{\text{wn}} \rightarrow 6 \frac{t}{\tau}, \quad (44)$$

$$\frac{m \langle (\Delta \mathbf{x})^2 \rangle}{k_B T \tau^2} \Big|_{\Gamma_1} \rightarrow 12 \frac{m}{\gamma \tau} \frac{t}{\tau}. \quad (45)$$

- (ii) For the case that one pole of $G(s)$ is located at $s=0$ and the other poles are located in the left half of the complex plane and not on the imaginary axis such as for colored noise with Γ_2 , $H(s)$ has a twofold pole at $s=0$. In the long-time limit, $H(t)$ goes to the residue of $H(s)e^{st}$ at $s=0$, which is $d[s^2 H(s)e^{st}]/ds|_{s=0} \sim sG(s)t|_{s=0} = a_1 t$ [see Eq. (20)]. This leads to $\langle (\Delta \mathbf{x})^2 \rangle(t) \rightarrow [v^2(0)a_1^2 + 3k_B T a_1(1-a_1)/m]t^2 \sim t^2$. The diffusion with a parabolic dependence of $\langle (\Delta \mathbf{x})^2 \rangle$ on t is an anomalous diffusion and called the ballistic diffusion. For Γ_2 , we obtain $\langle (\Delta \mathbf{x})^2 \rangle(t) \rightarrow [v^2(0) + 3k_B T C/m]t^2/(1+C)^2$ and

$$\frac{m \langle (\Delta \mathbf{x})^2 \rangle}{k_B T \tau^2} \Big|_{\Gamma_2} \rightarrow \frac{m v^2(0)/(k_B T) + 3C}{(1+C)^2} \left(\frac{t}{\tau} \right)^2. \quad (46)$$

- (iii) For the case that some poles of $G(s)$ are located on the imaginary axis but not at $s=0$ and the other poles are located in the left half of the complex plane such as for colored noise with Γ_3 , the poles on the imaginary axis lead to the oscillation of $H(t)$ with constant amplitudes. The long-time behavior is dominated by the pole of $H(s)$ at $s=0$ like in case (i). For Γ_3 , we get $G_3(s=0) = 2m/\gamma$, $\langle (\Delta \mathbf{x})^2 \rangle(t) \rightarrow 12k_B T t/\gamma \sim t$, and

$$\frac{m \langle (\Delta \mathbf{x})^2 \rangle}{k_B T \tau^2} \Big|_{\Gamma_3} \rightarrow 12 \frac{m}{\gamma \tau} \frac{t}{\tau}. \quad (47)$$

This is again the normal diffusion.

- (iv) For the case that the memory kernels $\Gamma(s)$ having branch points such as Eq. (25), $G_4(t) \sim (t/\tau)^{\lambda-2}$ for $0 < \lambda < 2$ in the long-time limit [see Eq. (27)]. $H_4(t)$ is obtained by the integral $H_4(t) = \int G_4(t)dt$. Putting $H_4(t)$ into Eq. (42), we have $\langle (\Delta \mathbf{x})^2 \rangle(t) \sim t^\lambda$. For $0 < \lambda < 1$, the diffusion is called the subdiffusion, while for $1 < \lambda < 2$ it is called the superdiffusion [1, 9, 11, 31, 32, 37–39].

Figure 4 shows the time evolution of the average displacement squared of the Brownian particle scaled by $k_B T \tau^2/m$. The results with white noise, Γ_1 ($B=0.5$), and Γ_2 are divided by 10. We see that the average displacement squared of the Brownian particle under white noise and colored noise with Γ_1 is linear in time in the long-time limit, whereas it is parabolic in time for colored noise with Γ_2 and is oscillating along a linear line in time for colored noise with Γ_3 .

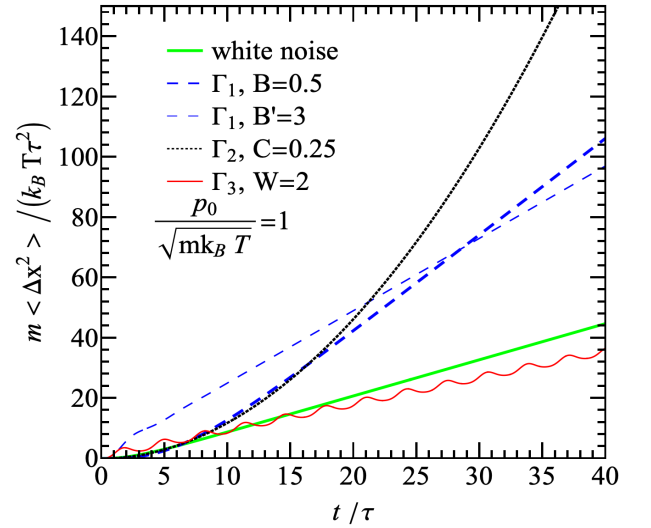


FIG. 4: The time evolution of the average displacement squared of the Brownian particle under white noise and colored noise with various memory kernels. The initial momentum of the Brownian particle is set to be $p_0 = \sqrt{m k_B T}$. The results with white noise, Γ_1 ($B=0.5$), and Γ_2 are divided by 10.

Finally, we discuss briefly the ergodicity in the Brownian motion with colored noise. The ergodicity states that the ensemble average of a variable equals its time average in the infinite-time limit. The necessary and sufficient condition of the ergodicity is given by Khinchin's theorem [11, 13], which declares that $C_O(t)/C_O(0)$ should vanish in the limit $t \rightarrow \infty$. $C_O(t) = \langle O(t)O(0) \rangle - \langle O(t) \rangle \langle O(0) \rangle$ is the autocorrelation of a stochastic variable $O(t)$. In the following, we examine $C_v(t)$ for various given memory kernels.

The derivation of $\langle \mathbf{v}(t) \cdot \mathbf{v}(0) \rangle$ from Eq. (11) is similar to that of $\langle v^2 \rangle(t)$. The result [11] is

$$C_v(t)/C_v(0) = G(t). \quad (48)$$

For white noise and colored noise with the first and fourth class of the memory kernels such as $\Gamma_1(t-t')$ and $\lim_{s \rightarrow 0} \Gamma_4(s) = \gamma(s\tau)^{\lambda-1}$ with $0 < \lambda < 2$, $G(t \rightarrow \infty) = 0$ and we have $\lim_{t \rightarrow \infty} C_v(t)/C_v(0) = 0$. The ergodicity holds.

For colored noise with other memory kernels such as Γ_2 and Γ_3 , the limits of $G_2(t)$ and $G_3(t)$ [see Eqs. (31) and (40)] do not go to zero for $t \rightarrow \infty$. Thus, $\lim_{t \rightarrow \infty} C_v(t)$ does not go to zero either. We see that velocities are always correlated, although the memory kernels have finite widths. In these two cases, the ergodicity is broken. In general, the ergodicity is broken when $G(s)$ has poles on the imaginal axis. This result does not depend on the initial state, which is different from the equilibration. As we have noticed, the equipartition theorem is broken for the cases with Γ_2 and Γ_3 , if the initial Brownian particles are out of thermal equilibrium [32].

B. Numerical calculations

In this subsection, we solve the Langevin equation, Eq. (1), numerically. Comparing to the conventional numerical method for solving ordinary differential equations, here we have to generate the series of noise from its time correlation [see Eqs. (2) and (3)]. The details of the generation of white and colored noise and the numerical method can be found in Ref. [30].

We have two purposes for performing the numerical calculations. First, we test our numerical computations by comparing the numerical results with the analytical ones to prepare a well-tested numerical code for solving the relativistic Langevin equation, which is introduced and investigated in the next section. Second, we want to calculate the momentum distribution of the Brownian particle in the long-time limit in the cases of colored noise with Γ_2 and Γ_3 , since obviously these distributions cannot be obtained analytically.

From the previous subsection, we notice that the Langevin equation, Eq. (1), can be nondimensionalized. Defining the dimensionless quantities $\tilde{\mathbf{p}} = m\mathbf{v}/\sqrt{mk_B T}$

and $\tilde{t} = t/\tau$, we obtain

$$\frac{d\tilde{\mathbf{p}}}{d\tilde{t}} = - \int_0^{\tilde{t}} d\tilde{t}' \tilde{\Gamma}(\tilde{t} - \tilde{t}') \tilde{\mathbf{p}}(\tilde{t}') + \tilde{\xi}(\tilde{t}), \quad (49)$$

where

$$\tilde{\Gamma}(\tilde{t} - \tilde{t}') = \frac{\tau^2}{m} \Gamma(t - t'), \quad (50)$$

which is dimensionless. Examples are plotted in the upper panel of Fig. 1. The dimensionless noise is $\tilde{\xi}(\tilde{t}) = \xi(t)\tau/\sqrt{mk_B T}$, with

$$\langle \tilde{\xi}_i(\tilde{t}) \tilde{\xi}_j(\tilde{t}') \rangle = \delta_{ij} \tilde{\Gamma}(\tilde{t} - \tilde{t}'). \quad (51)$$

Remember that τ is the decay timescale of the memory kernels. For the given memory kernels [see Eqs. (18), (22), and (32)] the only free parameter in Eq. (49) is $\gamma\tau/m$.

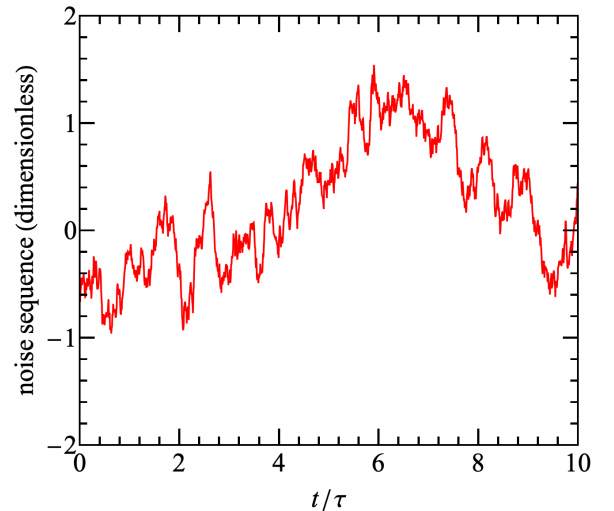


FIG. 5: Colored noise sequence.

Figure 5 shows one colored noise sequence in the case of Γ_3 with $W = 2$. Its time correlation function is shown in Fig. 6, where the numerical result agrees well with the given correlation function. Fifty thousand series of noise have been generated.

We have checked the time evolution of the average kinetic energy, displacement squared, and the time correlation of the velocity. The numerical results (not shown) agree well with the analytical ones presented in the previous subsection, see Figs. 1-4.

The momentum distributions of an ensemble of Brownian particles at long times are shown in Fig. 7 and compared with the Maxwell-Boltzmann distributions. For the case with Γ_3 , the distributions are calculated at the times when the average kinetic energy reaches its maximum (peak) as well as its minimum (trough), see Fig. 2. From Fig. 7 (a), we see that the distribution of the Brownian particle with Γ_3 at the peak agrees well with

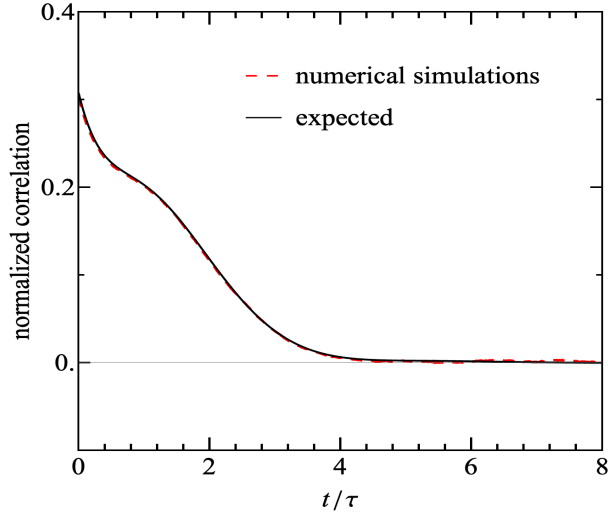


FIG. 6: Time correlation function of the noise with Γ_3 .

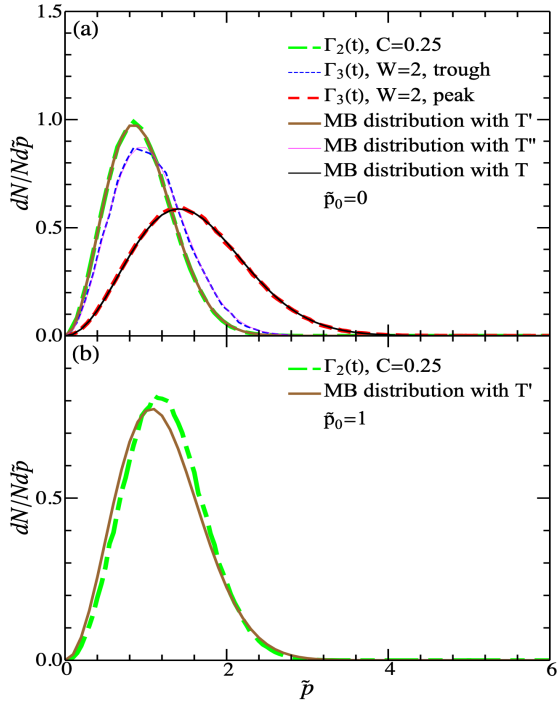


FIG. 7: The momentum distribution of the Brownian particle in the long-time limit.

the Maxwell-Boltzmann distribution with the temperature T of the surrounding matter. This is expected from the study in the previous subsection that the Brownian particle is in thermal equilibrium at peaks of the average kinetic energy in the long-time limit. It is also seen, as expected, that the momentum distributions of the Brownian particle with Γ_2 and with Γ_3 at the trough are not in thermal equilibrium with the surrounding matter. How-

ever, they look like the Maxwell-Boltzmann distributions with different “temperatures”. If so, then these “temperatures” can be obtained by the values of the average kinetic energy in the long-time limit according to Eq. (13). For the Brownian motion with Γ_2 , we have

$$\begin{aligned} \frac{3}{2}k_B T' &= \frac{1}{2}m \langle v^2 \rangle (t \rightarrow \infty) \\ &= \frac{3}{2}k_B T + \left[\frac{1}{2}mv^2(0) - \frac{3}{2}k_B T \right] G_2^2(t \rightarrow \infty) \\ &= \frac{3}{2}k_B T + \left[\frac{1}{2}mv^2(0) - \frac{3}{2}k_B T \right] \frac{1}{(1+C)^2} \quad (52) \end{aligned}$$

while for the Brownian motion with Γ_3 at the trough, we have

$$\begin{aligned} \frac{3}{2}k_B T'' &= \frac{3}{2}k_B T + \left[\frac{1}{2}mv^2(0) - \frac{3}{2}k_B T \right] \\ &\quad \times G_3^2(t \rightarrow \infty, \text{ at the trough}) \\ &= \frac{3}{2}k_B T + \left[\frac{1}{2}mv^2(0) - \frac{3}{2}k_B T \right] \\ &\quad \times \frac{1}{\left(1 + \frac{1}{2}\sqrt{\frac{W+1}{W+4}}\right)^2}. \quad (53) \end{aligned}$$

We plot the Maxwell-Boltzmann distributions with T' and T'' in Fig. 7 (a) and see agreements of these distributions with the numerical results. This is expected by looking at the unidimensional non-Gaussian indicator [32], since the initial velocity is set to be zero. The “temperature” that the Brownian particle feels is in some cases not the temperature of the matter, where the Brownian particle is suspended. Therefore, the attempt to use the Brownian particle to probe an unknown matter may become difficult because of possible occurrence of anomalous behaviors.

If the initial condition is nonthermal and the initial velocity is nonzero, the momentum distribution at a long time is expected to be non-Gaussian, if $G(t \rightarrow \infty) \neq 0$ [32]. In Fig. 7 (b), we show the momentum distribution of an ensemble of Brownian particles with Γ_2 and a fixed, nonzero initial momentum. The distribution is compared with the Maxwell-Boltzmann (Gaussian) distribution function with a “temperature” calculated from Eq. (52). We see the difference between two curves, which agrees with the expectation in Ref. [32].

III. THE LANGEVIN EQUATION OF RELATIVISTIC BROWNIAN PARTICLES

Assume that the matter, where the Brownian particle is suspended, remains at rest. Then, the Langevin equation, Eq. (1), can be extended to a form applied to relativistic particles [40–46],

$$\dot{\mathbf{p}}(t) = - \int_0^t dt' \Gamma(t-t') \frac{\mathbf{p}(t')c^2}{E(t')} + \boldsymbol{\xi}(t), \quad (54)$$

where \mathbf{p} is the momentum and $E = \sqrt{p^2 c^2 + m_0^2 c^4}$ is the energy of the Brownian particle with the rest mass m_0 . Its reduced form with white noise is

$$\dot{\mathbf{p}} = -\gamma \frac{\mathbf{p} c^2}{E} + \boldsymbol{\xi}. \quad (55)$$

The time correlation functions of the noise are same as those in Eqs. (2) and (5), respectively.

The formal solution of Eq. (55) reads

$$\mathbf{p}(t) = \mathbf{p}(t_0) e^{-\gamma \int_{t_0}^t \frac{ds' c^2}{E}} + \int_{t_0}^t ds e^{-\gamma \int_s^t \frac{ds' c^2}{E}} \boldsymbol{\xi}(s). \quad (56)$$

We then have $\langle \mathbf{p} \cdot \boldsymbol{\xi} \rangle = 3\alpha/2$. Taking the ensemble average of the scalar product of Eq. (55) with \mathbf{p} , we obtain

$$\frac{1}{2} \frac{d}{dt} \langle p^2 \rangle = -\gamma \langle \frac{p^2 c^2}{E} \rangle + \frac{3\alpha}{2}. \quad (57)$$

If the Brownian particle reaches the thermal equilibrium in the long-time limit, the left-hand side of the above equation vanishes and $\langle p^2 c^2 / E \rangle = 3k_B T$ by using the relativistic Boltzmann distribution $f = \exp[-E/(k_B T)]$. The same fluctuation-dissipation theorem as Eq. (6) is derived in the relativistic case. Therefore, we assume that the general fluctuation-dissipation theorem (3) is also valid for relativistic Brownian particles because a memory kernel having the δ -function form reduces the Langevin equation from Eq. (54) to Eq. (55) and the fluctuation-dissipation theorem from Eq. (3) to Eq. (6). We notice that from the assumption of the fluctuation-dissipation theorem, we can also derive that the relativistic Brownian particle under white noise will reach the thermal equilibrium in the long-time limit.

It is obvious that both Eqs. (54) and (55) are not linear differential-integral equations and thus cannot be solved analytically by using the Laplace transformation as performed in the nonrelativistic case. Even the solution (56) can only be calculated numerically, since E on the right-hand side of Eq. (56) is a function of p at times before t . Even though we can derive that the Brownian particle under white noise can reach the thermal equilibrium in the long-time limit, we cannot determine the behavior of the diffusion and ergodicity analytically.

In the following, we solve the Langevin equations, Eqs. (54) and (55), by using the numerical code mentioned and well tested in the previous section. The noise is approximately Gaussian [47]. We will study the equilibration, memory effect, diffusion, and ergodicity of Brownian particles under white noise and colored noise with the memory kernels Γ_1 , Γ_2 , and Γ_3 given in the previous section.

Like Eq. (49), the relativistic Langevin equation, Eq. (54), can also be nondimensionalized, when we define $\tilde{\mathbf{p}} = \mathbf{p}c/(k_B T)$, $\tilde{m}_0 = m_0 c^2/(k_B T)$, $\tilde{t} = t/\tau$, and $\tilde{\boldsymbol{\xi}} = \boldsymbol{\xi} \tau c/(k_B T)$. We have then

$$\frac{d\tilde{\mathbf{p}}}{d\tilde{t}} = - \int_0^{\tilde{t}} d\tilde{t}' \tilde{\Gamma}(\tilde{t} - \tilde{t}') \frac{\tilde{\mathbf{p}}(\tilde{t}')}{\sqrt{\tilde{p}^2 + \tilde{m}_0^2}} + \tilde{\boldsymbol{\xi}}(\tilde{t}), \quad (58)$$

where

$$\tilde{\Gamma}(\tilde{t} - \tilde{t}') = \frac{\tau^2 c^2}{k_B T} \Gamma(t - t') \quad (59)$$

and

$$\langle \tilde{\xi}_i(\tilde{t}) \tilde{\xi}_j(\tilde{t}') \rangle = \delta_{ij} \tilde{\Gamma}(\tilde{t} - \tilde{t}'). \quad (60)$$

τ is the decay timescale in the given memory kernels. Looking at the memory kernels Γ_1 , Γ_2 , and Γ_3 in Eqs. (18), (22), and (32), we find that \tilde{m}_0 and $\gamma \tau c^2/(k_B T)$ are the free parameters in Eq. (58). Note that $\omega \tau$ in Γ_3 is not an additional parameter, since $\omega \tau$ (or W) is fixed by $\gamma \tau/m_0$ in Eq. (39), where we replace m by m_0 . We also realize that τ does not exist in the Langevin equation with white noise, Eq. (55). In this case, we define $\tau = k_B T/(\gamma c^2)$.

Figure 8 shows the time evolution of the average kinetic energy of the relativistic Brownian particle, $E_k = E - m_0 c^2$ scaled by $k_B T$, under colored noise with Γ_1 . The initial momentum of the Brownian particle is zero.

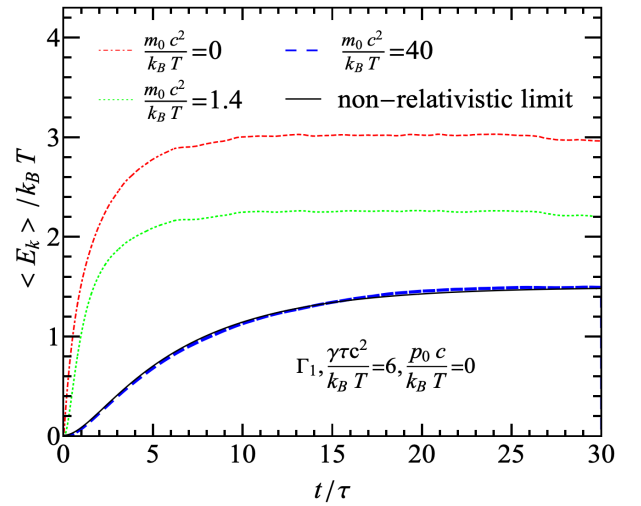


FIG. 8: The time evolution of the average kinetic energy of the relativistic Brownian particle under colored noise with Γ_1 and with various rest masses. The initial momentum of the particle is set to be zero.

The parameter $\gamma \tau c^2/(k_B T)$ is set to be 6. For $\tau = 1$ fm/c and $T = 300$ MeV, $\gamma/2$ is consistent with the drag coefficient in the Brownian motion of charm quarks in the quark-gluon plasma created in relativistic heavy-ion collisions [17, 22, 27, 48–53]. We vary the rest mass of the Brownian particle to see the relativistic effect and to check the numerical calculations.

We see that in the long-time limit, the average kinetic energy increases from the nonrelativistic limit, $3k_B T/2$, to the ultrarelativistic limit, $3k_B T$. All the final values with different masses agree with those according to the equipartition theorem, which indicates that the Brownian particle under colored noise with Γ_1 reaches the thermal equilibrium with its surrounding matter. The numerical result of the relativistic Langevin equation with

a large mass $\tilde{m}_0 = 40$ is compared with the analytical one of the nonrelativistic Langevin equation. The perfect agreement demonstrates the solid numerical calculations.

The time evolution of the average kinetic energy of the relativistic Brownian particle with mass $\tilde{m}_0 = 1.4$ under white noise and colored noise with the memory kernels Γ_1 , Γ_2 , and Γ_3 are depicted in Fig. 9. The initial

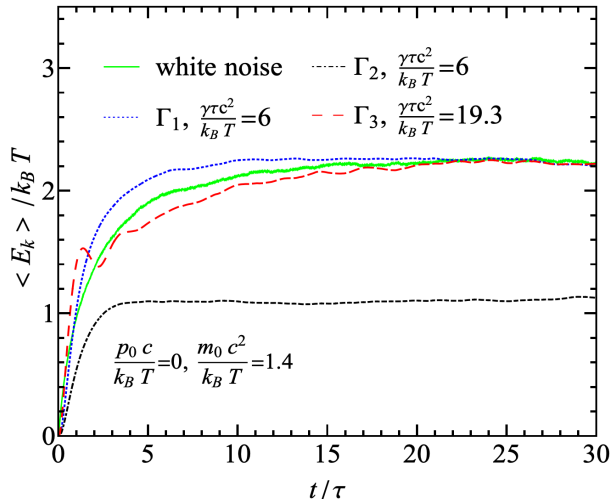


FIG. 9: Same as Fig. 8 but under white noise and colored noise with various memory kernels.

momentum is zero. The curve of Γ_1 is the same as that in Fig. 8. For Γ_3 with $W = 2$, we obtain $\gamma\tau/m_0 = 13.8$ according to Eq. (39) by replacing m by m_0 . Thus, we have $\gamma\tau c^2 / (k_B T) = 19.3$ for $\tilde{m}_0 = 1.4$.

From Fig. 9, we see that the average kinetic energy of the Brownian particle under white noise and colored noise with Γ_1 and Γ_3 approaches the same value in the long-time limit, which is the value according to the equipartition theorem. The oscillating behavior in the nonrelativistic limit with Γ_3 does not occur here. Remember that Eq. (39) is a strict condition for the oscillating behavior in the nonrelativistic case, which is not necessarily the same one met in the relativistic case.

The long-time limit of the average kinetic energy of the Brownian particle with Γ_2 is smaller than that with other memory kernels. The anomalous behavior already seen in the nonrelativistic case appears in the relativistic case too. We want to know whether we can make use of the formulas derived in the nonrelativistic limit in the previous section to analyze the results achieved in the relativistic case. From Eq. (13), we get the average kinetic energy in the long-time limit,

$$\frac{\langle E_k \rangle_{|t \rightarrow \infty}}{k_B T} = \frac{\langle E_k \rangle_{|t=0}}{k_B T} \frac{1}{(1+C)^2} + \frac{3}{2} \left[1 - \frac{1}{(1+C)^2} \right], \quad (61)$$

where $E_k = p^2/(2m)$ and $C = \gamma\tau/(4m)$. We use this formula and replace m by m_0 . For $p_0 = 0$, $\gamma\tau c^2 / (k_B T) =$

6, and $\tilde{m}_0 = 1.4$, we obtain $\langle E_k \rangle_{|t \rightarrow \infty} / (k_B T) = 1.15$, which agrees with the numerical result seen in Fig. 9.

The memory effect of the initial momentum is shown in Fig. 10. In these calculations, the initial momentum is

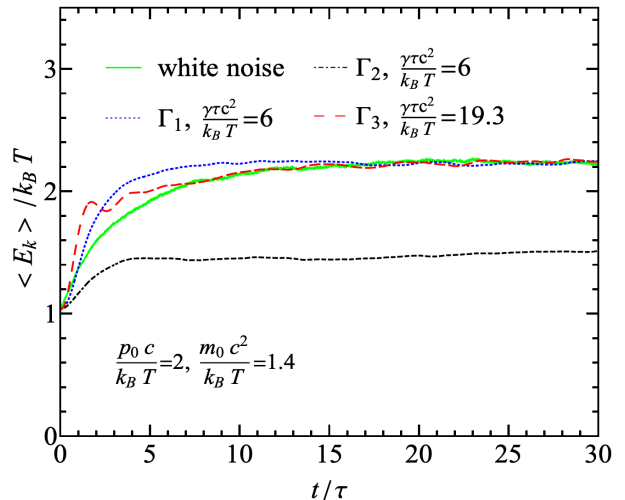


FIG. 10: Same as Fig. 9, but the initial momentum of the particle is set to be $p_0 c / (k_B T) = 2$.

set to be $p_0 c / (k_B T) = 2$. By comparing with Fig. 9, we see that while the long-time limit of the average kinetic energy of the relativistic Brownian particle under white noise and colored noise with Γ_1 and Γ_3 do not show any dependence of the initial momentum, it does appear for the particle with Γ_2 . Using the formula in the nonrelativistic limit (61), we obtain $\langle E_k \rangle_{|t \rightarrow \infty} / (k_B T) = 1.48$ for $p_0 c / (k_B T) = 2$, which also agrees with the numerical result seen in Fig. 10.

We depict the time evolution of the average displacement squared, scaled by $\tau^2 c^2$, in Fig. 11. The behaviors of the diffusion are the same as in the nonrelativistic limit. The particle diffusion under white noise and colored noise with Γ_1 and Γ_3 are normal, while it is ballistic for the particle with Γ_2 . Using the formulas in the nonrelativistic limit Eqs. (44)-(47) times $k_B T / (m_0 c^2)$,

$$\frac{\langle (\Delta \mathbf{x})^2 \rangle_{| \text{wn}}}{\tau^2 c^2} \rightarrow 6 \frac{k_B T}{m_0 c^2} \frac{t}{\tau}, \quad (62)$$

$$\frac{\langle (\Delta \mathbf{x})^2 \rangle_{| \Gamma_1, \Gamma_3}}{\tau^2 c^2} \rightarrow 12 \frac{k_B T}{\gamma\tau c^2} \frac{t}{\tau}, \quad (63)$$

$$\frac{\langle (\Delta \mathbf{x})^2 \rangle_{| \Gamma_2}}{\tau^2 c^2} \rightarrow \frac{k_B T}{m_0 c^2} \frac{p_0^2 / (m_0 k_B T) + 3C}{(1+C)^2} \left(\frac{t}{\tau} \right)^2 \quad (64)$$

we compare these nonrelativistic results with the relativistic ones. We find perfect agreements for colored noise with Γ_1 and Γ_3 , an approximate agreement for white noise, and a difference of almost a factor of 2 for colored noise with Γ_2 .

Finally, we calculate the autocorrelation function of momentum at different times to study the validity of the

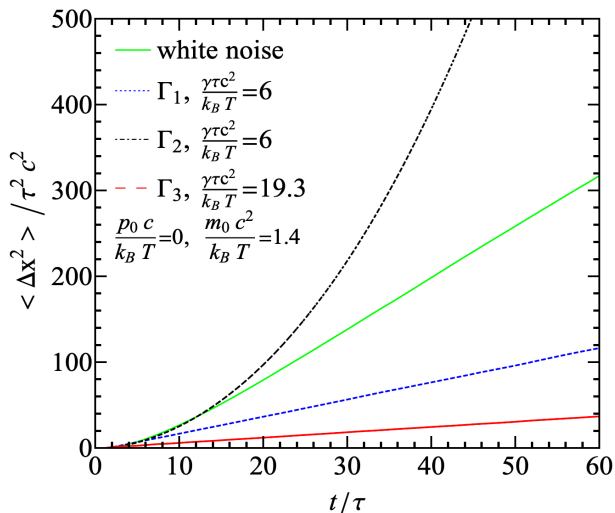


FIG. 11: The time evolution of the average displacement squared of the relativistic Brownian particle under white noise and colored noise with various memory kernels. The initial momentum of the particle is set to be $p_0 = 0$.

ergodicity in the motion of relativistic Brownian particles. Figure 12 shows the numerical results for the initial momentum $\tilde{p}_0 = 1$ with a random direction. The mo-

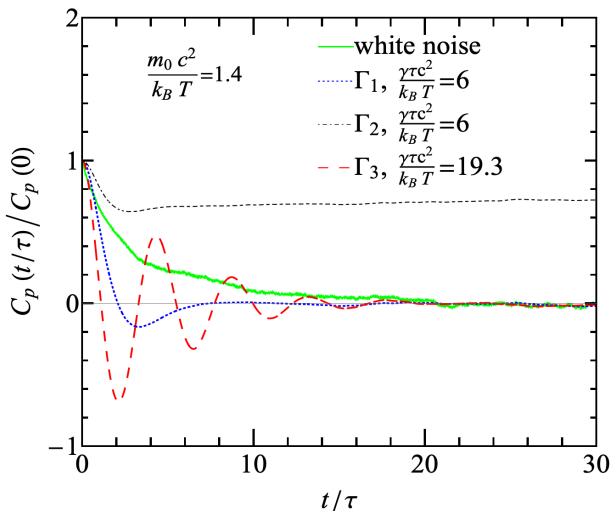


FIG. 12: The autocorrelation function of momentum of the relativistic Brownian particle under white noise and colored noise with various memory kernels.

mentum is scaled by $k_B T/c$. We clearly see that C_p with Γ_2 is nonzero in the long-time limit, while the other three correlations approach zero. Therefore, the motion with Γ_2 breaks the validity of the ergodicity, while the motions under white noise and colored noise with Γ_1 and Γ_3 hold the ergodicity.

IV. SUMMARY

In this paper, we solved analytically the generalized Langevin equation of nonrelativistic Brownian particles with the memory kernel and colored noise by employing the Laplace transformation technique. According to the position of the singularities of the response function $G(s)$, the memory kernels are classified to four categories, which result in different behaviors of the thermal equilibrium, the memory effect, the particle diffusion, and the ergodicity. Specifically, the first category includes the cases that all the poles of $G(s)$ are located in the left half of the complex plane but not on the imaginary axis. In the long-time limit, the Brownian particle approaches thermal equilibrium with the surrounding matter, has no memory of the initial state, and diffuses normally. The ergodicity holds. The second category includes the cases that one pole is located on the imaginary axis and specially at the origin $s = 0$ and the other poles are located in the left half of the complex plane. Usually, the Brownian particle cannot reach the equilibrium with the surrounding matter, but will reach an equilibrium with a different temperature rather than that of the surrounding matter, if the initial velocity is zero. This temperature as well as the average kinetic energy of the Brownian particle depend on its initial state, which shows the memory effect. The particle diffusion is ballistic and the ergodicity is broken. The third category includes the cases that some poles in pairs are located on the imaginary axis but not at the origin and the other poles are located in the left half of the complex plane. The Brownian particle approaches and departs from the thermal equilibrium with the surrounding matter periodically. The amplitude of the oscillation in the average kinetic energy depends on the initial state, which is again the memory effect. The diffusion of the Brownian particle is normal, but the ergodicity is broken. The fourth and last category includes the memory kernels with the form $\lim_{s \rightarrow 0} \Gamma(s) = \gamma(s\tau)^{\lambda-1}$, which has a branch point at $s = 0$. For $0 < \lambda < 2$, $G(t \rightarrow \infty)$ goes to zero. The long-time behaviors of the Brownian particle are the following. The particle approaches the thermal equilibrium with the surrounding matter and has no memory of the initial state. For $0 < \lambda < 1$, the diffusion is the subdiffusion, while it is superdiffusion for $1 < \lambda < 2$. The ergodicity holds. For $\lambda > 2$, the branch point is replaced by the pole at $s = 0$ in the long-time limit. The behaviors of the Brownian particle are the same as those in the second category.

For relativistic Brownian particles, the Langevin equation cannot be solved analytically because of the nonlinearity. Therefore, we do not have a general conclusion about the behavior of the thermal equilibrium, memory effects, diffusion, and ergodicity for any given memory kernel. On the other hand, we solved the relativistic Langevin equation numerically for three typical memory kernels chosen as the examples in the nonrelativistic case. Similar results as obtained in the nonrelativistic case for the first and second categories of memory kernels are also

seen in the relativistic case. In other words, there are indeed memory kernels, with which the relativistic Brownian particle cannot reach thermal equilibrium, has memory effects of the initial state, and diffuses anomalously. Its motion breaks the ergodicity. Moreover, by regarding the relativistic particle as the nonrelativistic one (by replacing the mass by the rest mass), the average kinetic energy and the average displacement squared (except for one case with Γ_2) can be well described by the formulas derived in the nonrelativistic case.

Persistent nonequilibrium effects in Brownian motions may challenge the probe of an unknown matter by using a Brownian particle. On the other hand, our present investigation may give rise to think about the memory effect and anomalous diffusion of heavy quarks in the quark-gluon plasma created in relativistic heavy-ion collisions.

Acknowledgments

This work was financially supported by the National Natural Science Foundation of China under Grants No. 11890710, No. 11890712, and No. 12035006, the Ministry of Science and Technology under Grant No. 2020YFE0202001. C.G. acknowledges support by the Deutsche Forschungsgemeinschaft (DFG) through the grant CRC-TR 211 “Strong-interaction matter under extreme conditions.”

Appendix A: Laplace transformation

The Laplace transform of a function $f(t)$ is defined as

$$L[f(t)] = \int_0^t dt f(t) e^{-st} \equiv f(s), \quad (\text{A1})$$

where s is a complex variable. The inverse transform is

$$L^{-1}[f(s)] = \frac{1}{2\pi i} \int_{\beta-i\infty}^{\beta+i\infty} ds f(s) e^{st}. \quad (\text{A2})$$

Some useful properties of the Laplace transformation are listed below:

$$L\left[\frac{df(t)}{dt}\right] = sf(s) - f(t=0), \quad (\text{A3})$$

$$L\left[\int_0^t dt' f(t-t')g(t')\right] = f(s)g(s), \quad (\text{A4})$$

$$L\left[\frac{d^2f(t)}{dt^2}\right] = s^2f(s) - sf(t=0) - \frac{df(t)}{dt}(t=0) \quad (\text{A5})$$

We now derive Eq. (13) from Eq. (12)

$$\begin{aligned} \langle v^2 \rangle(t) &= v^2(0)G^2(t) + \frac{3k_B T}{m^2} \int_0^t dt' G(t-t') \\ &\quad \times \int_0^t dt'' G(t-t'')\Gamma(t''-t'). \end{aligned}$$

Because the integrals for $t'' \geq t'$ and $t'' \leq t'$ are same, we rewrite the above equation to

$$\begin{aligned} \langle v^2 \rangle(t) &= v^2(0)G^2(t) + \frac{3k_B T}{m^2} 2 \int_0^t dt' G(t-t') \\ &\quad \times \int_0^{t'} dt'' G(t-t'')\Gamma(t''-t')\theta(t''-t') \quad (\text{A6}) \end{aligned}$$

By $\tau = t'' - t'$, we have

$$\begin{aligned} &\int_0^t dt'' G(t-t'')\Gamma(t''-t')\theta(t''-t') \\ &= \int_{-t'}^{t-t'} d\tau G(t-t'-\tau)\Gamma(\tau)\theta(\tau) \\ &= \int_0^{t-t'} d\tau G(t-t'-\tau)\Gamma(\tau) \\ &= L^{-1}\left\{L\left[\int_0^{t-t'} d\tau G(t-t'-\tau)\Gamma(\tau)\right]\right\} \\ &= L^{-1}[G(s)\Gamma(s)]. \end{aligned}$$

Since $G(s) = 1/[s + \Gamma(s)/m]$ and $G(t=0) = 1$, we get

$$G(s)\Gamma(s) = m[sG(s) - G(t=0)] = mL\left[\frac{dG(t-t')}{d(t-t')}\right]$$

and

$$L^{-1}[G(s)\Gamma(s)] = m \frac{dG(t-t')}{d(t-t')} = -m \frac{dG(t-t')}{dt'}.$$

Putting this in Eq. (A6), we finally obtain

$$\begin{aligned} \langle v^2 \rangle(t) &= v^2(0)G^2(t) - \frac{3k_B T}{m} 2 \int_0^t dt' G(t-t') \frac{dG(t-t')}{dt'} \\ &= v^2(0)G^2(t) + \frac{3k_B T}{m} [1 - G^2(t)]. \end{aligned}$$

-
- [1] Z.-W. Bai, J.-D. Bao, and Y.-L. Song, Phys. Rev. E **72**, 061105 (2005), URL <https://link.aps.org/doi/10.1103/PhysRevE.72.061105>.
[2] J.-D. Bao, Y.-L. Song, Q. Ji, and Y.-Z. Zhuo, Phys. Rev.

- E **72**, 011113 (2005), URL <https://link.aps.org/doi/10.1103/PhysRevE.72.011113>.
[3] R. M. S. Ferreira, M. V. S. Santos, C. C. Donato, J. S. Andrade, and F. A. Oliveira, Phys. Rev. E **86**,

- 021121 (2012), URL <https://link.aps.org/doi/10.1103/PhysRevE.86.021121>.
- [4] W. Wang, A. G. Cherstvy, A. V. Chechkin, S. Thapa, F. Seno, X. Liu, and R. Metzler, *Journal of Physics A: Mathematical and Theoretical* **53**, 474001 (2020).
- [5] A. G. Cherstvy, W. Wang, R. Metzler, and I. M. Sokolov, *Phys. Rev. E* **104**, 024115 (2021), URL <https://link.aps.org/doi/10.1103/PhysRevE.104.024115>.
- [6] W. Wang, R. Metzler, and A. G. Cherstvy, *Physical Chemistry Chemical Physics* **24**, 18482 (2022).
- [7] M. Magdziarz and A. Weron, *Phys. Rev. E* **84**, 051138 (2011), URL <https://link.aps.org/doi/10.1103/PhysRevE.84.051138>.
- [8] J.-D. Bao, Y.-Z. Zhuo, F. A. Oliveira, and P. Hänggi, *arXiv e-prints cond-mat/0605093* (2006), cond-mat/0605093.
- [9] P. Siegle, I. Goychuk, and P. Hänggi, *Phys. Rev. Lett.* **105**, 100602 (2010), URL <https://link.aps.org/doi/10.1103/PhysRevLett.105.100602>.
- [10] J.-D. Bao, Y. Zhou, and K. Lü, *Phys. Rev. E* **74**, 041125 (2006), URL <https://link.aps.org/doi/10.1103/PhysRevE.74.041125>.
- [11] L. C. Lapas, R. Morgado, M. H. Vainstein, J. M. Rubí, and F. A. Oliveira, *Phys. Rev. Lett.* **101**, 230602 (2008), URL <https://link.aps.org/doi/10.1103/PhysRevLett.101.230602>.
- [12] J.-D. Bao, P. Hänggi, and Y.-Z. Zhuo, *Phys. Rev. E* **72**, 061107 (2005), URL <https://link.aps.org/doi/10.1103/PhysRevE.72.061107>.
- [13] M. H. Lee, *Phys. Rev. Lett.* **98**, 190601 (2007), URL <https://link.aps.org/doi/10.1103/PhysRevLett.98.190601>.
- [14] S. Li, W. Xiong, and R. Wan, *Eur. Phys. J. C* **80**, 1113 (2020), 2012.02489.
- [15] J.-H. Liu, S. K. Das, V. Greco, and M. Ruggieri, *Phys. Rev. D* **103**, 034029 (2021), 2011.05818.
- [16] M. Ruggieri, Pooja, J. Prakash, and S. K. Das, *Phys. Rev. D* **106**, 034032 (2022), 2203.06712.
- [17] G. D. Moore and D. Teaney, *Phys. Rev. C* **71**, 064904 (2005), hep-ph/0412346.
- [18] S. Li and J. Liao, *Eur. Phys. J. C* **80**, 671 (2020), 1912.08965.
- [19] Y. Akamatsu, T. Hatsuda, and T. Hirano, *Phys. Rev. C* **79**, 054907 (2009), URL <https://link.aps.org/doi/10.1103/PhysRevC.79.054907>.
- [20] S. K. Das, F. Scardina, S. Plumari, and V. Greco, *Phys. Lett. B* **747**, 260 (2015), 1502.03757.
- [21] Y. Sun, G. Coci, S. K. Das, S. Plumari, M. Ruggieri, and V. Greco, *Phys. Lett. B* **798**, 134933 (2019), 1902.06254.
- [22] X. Dong and V. Greco, *Prog. Part. Nucl. Phys.* **104**, 97 (2019).
- [23] S. Cao, G.-Y. Qin, and S. A. Bass, *Phys. Rev. C* **88**, 044907 (2013), 1308.0617.
- [24] S. Cao, G.-Y. Qin, and S. A. Bass, *Nucl. Phys. A* **931**, 569 (2014), 1408.0503.
- [25] S. Cao, G.-Y. Qin, and S. A. Bass, *Phys. Rev. C* **92**, 024907 (2015), 1505.01413.
- [26] S. K. Das, F. Scardina, S. Plumari, and V. Greco, *Phys. Rev. C* **90**, 044901 (2014), 1312.6857.
- [27] H. van Hees, V. Greco, and R. Rapp, *Phys. Rev. C* **73**, 034913 (2006), nucl-th/0508055.
- [28] R. Kubo, *Reports on Progress in Physics* **29**, 255 (1966), URL <https://doi.org/10.1088/0034-4885/29/1/306>.
- [29] C. Greiner and S. Leupold, *Annals Phys.* **270**, 328 (1998), hep-ph/9802312.
- [30] Z. Xu and C. Greiner, *Phys. Rev. D* **62**, 036012 (2000), hep-ph/9910562.
- [31] L. C. Lapas, R. Morgado, A. L. Penna, and F. A. Oliveira, *Acta Physica Polonica B* **46** (2015).
- [32] L. Lapas, I. Costa, M. Vainstein, and F. Oliveira, *Europhysics Letters* **77**, 37004 (2007).
- [33] B. Schüller, A. Meistrenko, H. Van Hees, Z. Xu, and C. Greiner, *Annals Phys.* **412**, 168045 (2020), 1905.09652.
- [34] J. Schmidt, A. Meistrenko, H. van Hees, Z. Xu, and C. Greiner, *Phys. Rev. E* **91**, 032125 (2015), 1407.6528.
- [35] M. T. M. T. R. Kubo, N. Hashitsume, *Statistical physics II: Nonequilibrium statistical mechanics*, Springer Series in Solid-State Sciences (Springer Berlin, Heidelberg, 1985), 1st ed., ISBN 3540114610, 9783540114611, URL <http://gen.lib.rus.ec/book/index.php?md5=6064f44bc0a8c3e9c5a4c24ca060b194>.
- [36] H. J. Haubold, A. M. Mathai, and R. K. Saxena, *Journal of applied mathematics* **2011** (2011).
- [37] K. Lü and J.-D. Bao, *Phys. Rev. E* **72**, 067701 (2005), URL <https://link.aps.org/doi/10.1103/PhysRevE.72.067701>.
- [38] J. M. Porrà, K.-G. Wang, and J. Masoliver, *Phys. Rev. E* **53**, 5872 (1996), URL <https://link.aps.org/doi/10.1103/PhysRevE.53.5872>.
- [39] B. Li and J. Wang, *Phys. Rev. Lett.* **91**, 044301 (2003), URL <https://link.aps.org/doi/10.1103/PhysRevLett.91.044301>.
- [40] F. Debbasch, K. Mallick, and J.-P. Rivet, *Journal of Statistical Physics* **88**, 945 (1997).
- [41] F. Debbasch and J.-P. Rivet, *Journal of Statistical Physics* **90**, 1179 (1998).
- [42] C. Chevalier and F. Debbasch, *Journal of Mathematical Physics* **49**, 043303 (2008).
- [43] J. Dunkel and P. Hänggi, *Phys. Rev. E* **71**, 016124 (2005), cond-mat/0411011.
- [44] J. Dunkel and P. Hänggi, *Phys. Rept.* **471**, 1 (2009), 0812.1996.
- [45] P. S. Pal and S. Deffner, *New Journal of Physics* **22**, 073054 (2020), URL <https://doi.org/10.1088/2F1367-2630/22Fab9ce6>.
- [46] J. Dunkel and P. Hänggi, *Phys. Rev. E* **72**, 036106 (2005), URL <https://link.aps.org/doi/10.1103/PhysRevE.72.036106>.
- [47] J. Dunkel and P. Hänggi, *Phys. Rev. E* **74**, 051106 (2006), URL <https://link.aps.org/doi/10.1103/PhysRevE.74.051106>.
- [48] S. Cao, G.-Y. Qin, and S. A. Bass, *Phys. Rev. C* **92**, 054909 (2015), 1505.01869.
- [49] Y. Akiba et al. (2015), 1502.02730.
- [50] A. Adare et al. (PHENIX), *Phys. Rev. Lett.* **98**, 172301 (2007), nucl-ex/0611018.
- [51] S. Acharya et al. (ALICE), *Phys. Lett. B* **813**, 136054 (2021), 2005.11131.
- [52] D. Banerjee, S. Datta, R. Gavai, and P. Majumdar, *Phys. Rev. D* **85**, 014510 (2012), 1109.5738.
- [53] H.-T. Ding, A. Francis, O. Kaczmarek, F. Karsch, H. Satz, and W. Soeldner, *Phys. Rev. D* **86**, 014509 (2012), URL <https://link.aps.org/doi/10.1103/PhysRevD.86.014509>.